

Supporting Information

Interfacial Superassembly of Grape-like MnO-Ni@C Frameworks for Superior Lithium Storage

Chuanxin Hou,[†], ^{‡#} Jun Wang,^{†#} Weibin Zhang,[†] Jiajia Li,[†] Runhao Zhang,[‡] Junjie Zhou,[‡] Yuqi Fan,[§] Dajian Li,[⊥] Feng Dang,^{†} Jiaqing Liu[‡] Yong Li,[‡] Kang Liang,[▽] and Biao Kong^{‡*}*

[†]Key Laboratory for Liquid-Solid Structural Evolution 1and Processing of Materials (Ministry of Education), Shandong University, Jinan 250061, P. R. China

[‡]Department of Chemistry, Laboratory of Advanced Materials, Fudan University, Shanghai 200433, P. R. China

[§]Institute of Environment and Ecology, Shandong Normal University, Jinan 250014, P. R. China

[⊥]Institute for Applied Materials-Applied Materials Physics (IAM-AWP), Karlsruhe Institute of Technology (KIT), Hermann-von-Helmholtz-Platz 1, 76344, Eggenstein-Leopoldshafen, Germany

[▽]School of Chemical Engineering and Graduate School of Biomedical Engineering, The University of New South Wales, NSW 2052, Australia.

These authors contributed equally.

Corresponding Author

*E-mail: bkong@fudan.edu.cn (B.K.); dangfeng@sdu.edu.cn (F.D.)

Contents

Figure S1. XRD pattern of MCO ₃	Page 3
Figure S2. SEM images of MCO ₃ /ager gel matrix precursor: 5% Ni, 10% Ni and 15% Ni (c)	Page 4
Figure S3. SEM images of MnO-Ni5@C, MnO-Ni10 and MnO-Ni15@C.....	Page 5
Figure S4. Charge-discharge profiles of MnO-Ni5@C and MnO-Ni15@C electrodes at the current density of 0.1 A g ⁻¹	Page 6
Figure S5. Charge-discharge profiles of MnO-Ni10@C electrodes at different current densities	Page 7
Figure S6 The corresponding selected charge-discharge profiles of MnO-Ni10@C at 1.0 A g ⁻¹ for a ultralong cycle life of 2100 cycles.....	Page 8
Figure S7. Cycling performance and coulombic efficiency of MnO-Ni5@C and MnO-Ni15@C electrodes at current density of 0.1 A g ⁻¹	Page 9
Figure S8. CV curves at differet scan rates from 0.1-1.5 mV s ⁻¹ of MnO-Ni0@C and MnO-Ni10@C electrodes.....	Page 10
Figure S9. Current responses plotted against different scan rates of MnO-Ni10@C electrodes at different potentials for cathodic scans and anodic scans.....	Page 11
Figure S10. SEM images of MnO-Ni5@C and MnO-Ni15@C electrodes after 200 and 100 cycles, respectively.....	Page 12
Figure S11. The calculated room temperature phase diagram of Ni-Mn-O system.	Page 13
Figure S12. Calculated MnO-Ni vertical section of the Ni-Mn-O system.....	Page 14
Table S1. Comparison of the electrochemical performance of the transition metal oxides electrodes.....	Page 15

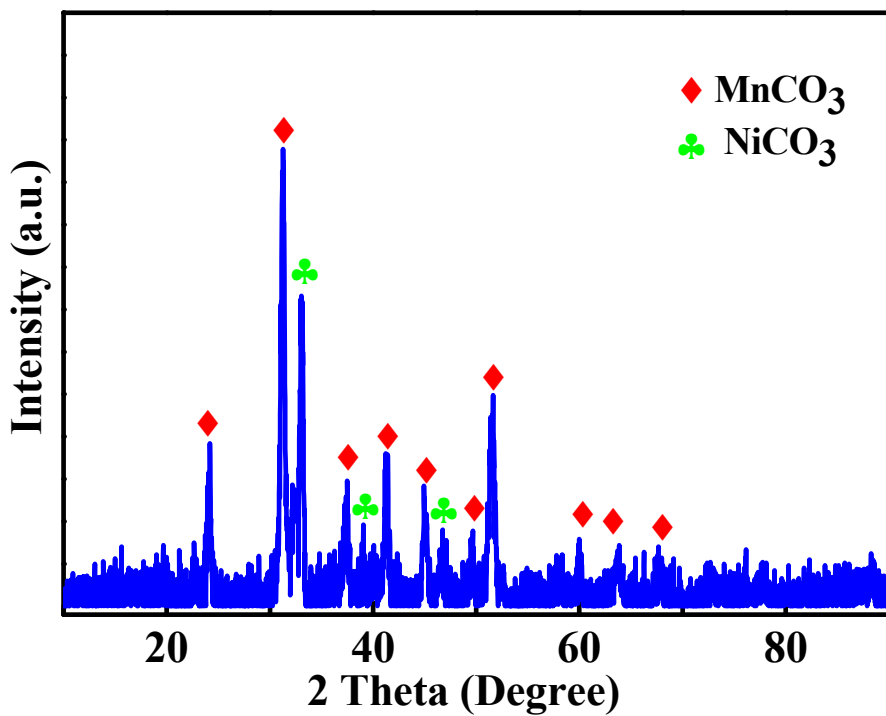


Figure S1. XRD pattern of MCO₃.

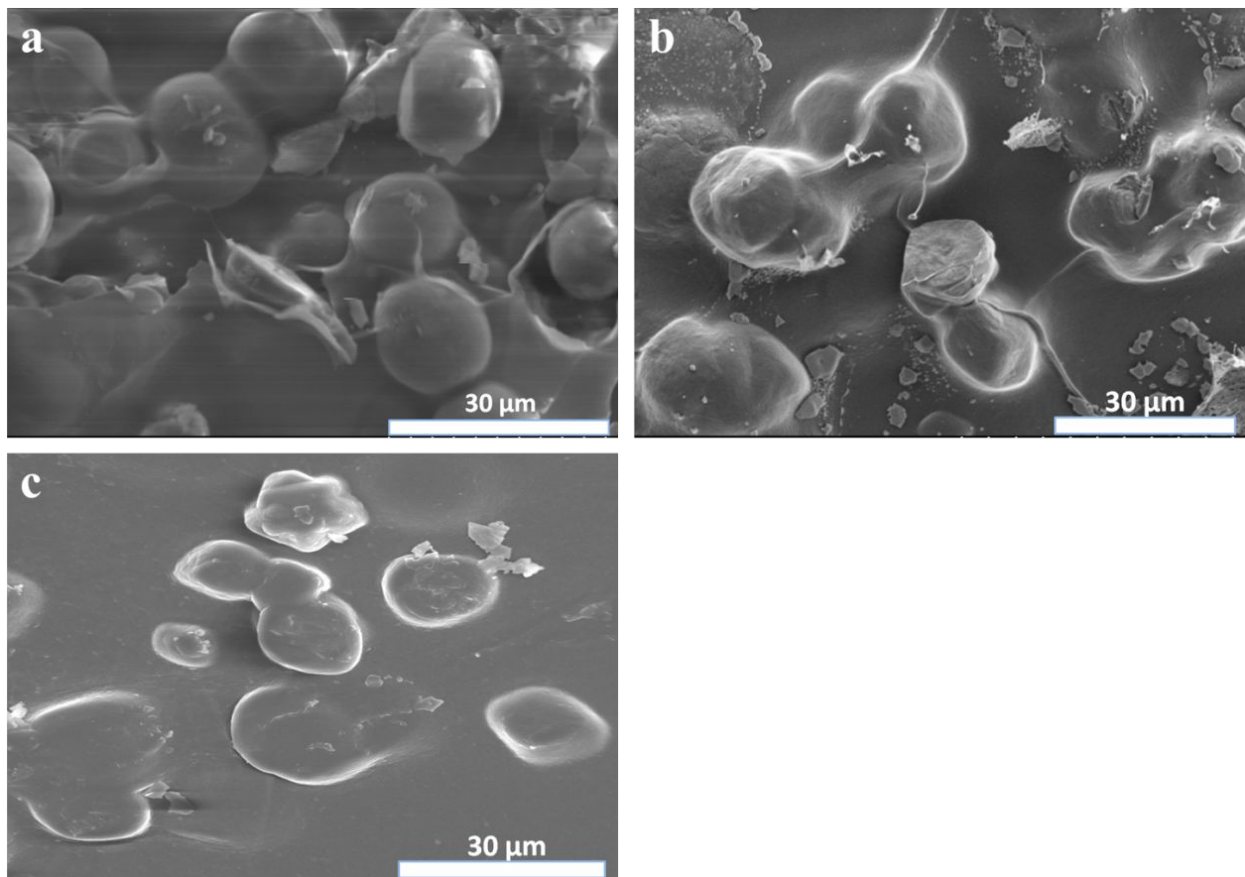


Figure S2. SEM images of MCO_3 /ager gel matrix precursor: 5% (a); 10% (b) and 15% Ni (c).

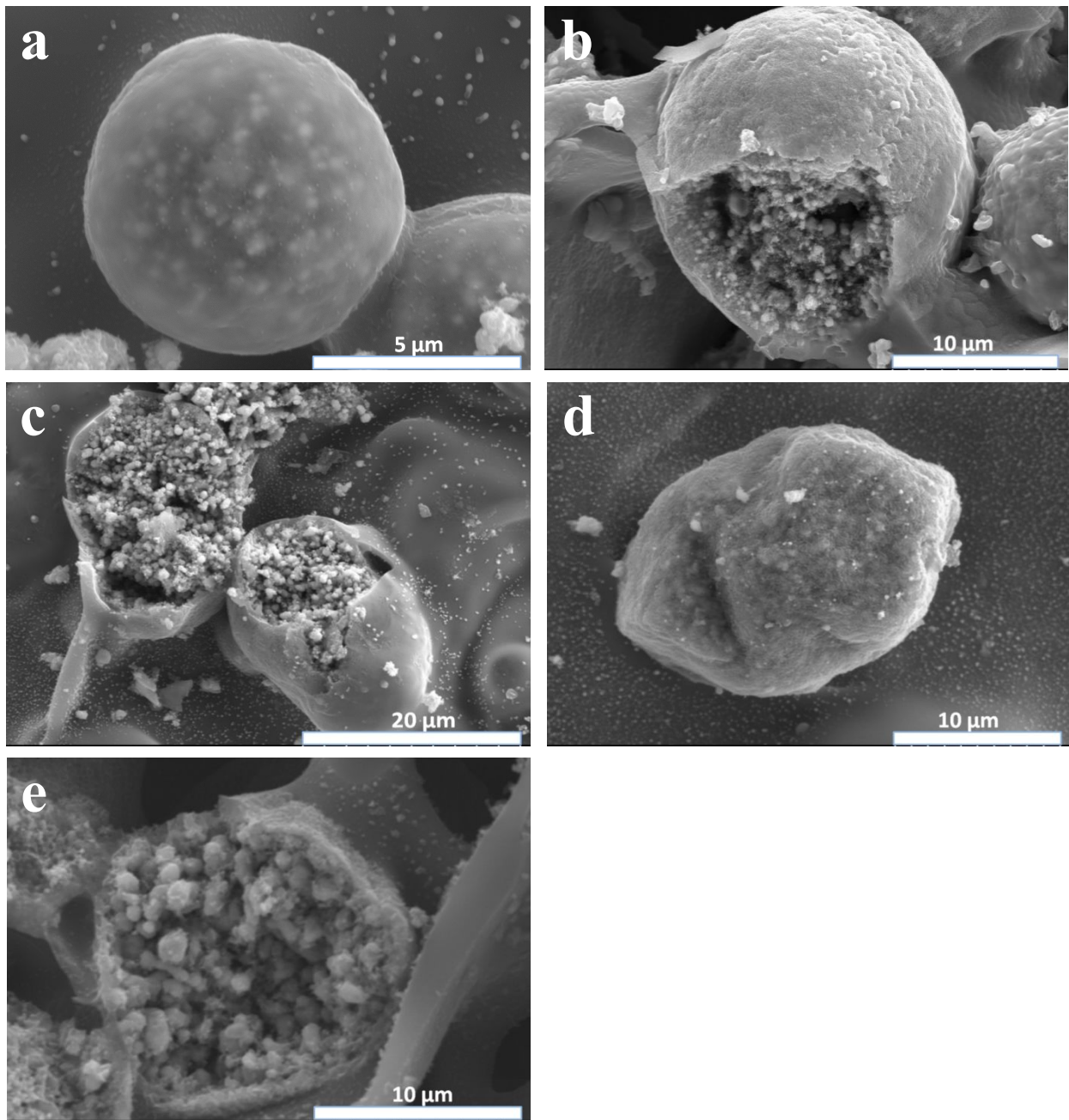


Figure S3. SEM images of MnO-Ni5@C (a, b), MnO-Ni10 (c) and MnO-Ni15@C (d, e).

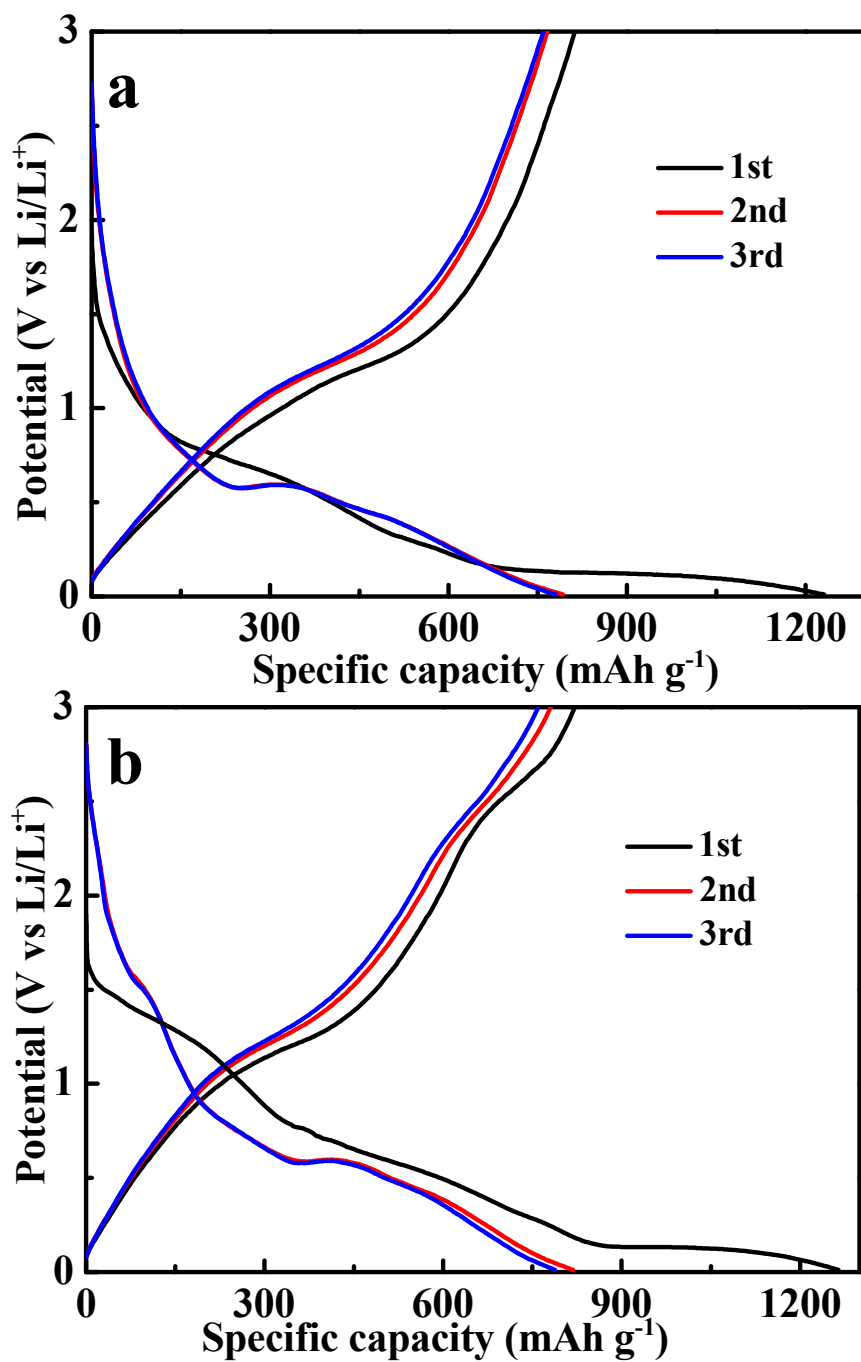


Figure S4. Charge-discharge profiles of MnO-Ni5@C (a) and MnO-Ni15@C (b) electrodes at the current density of 0.1 A g⁻¹.

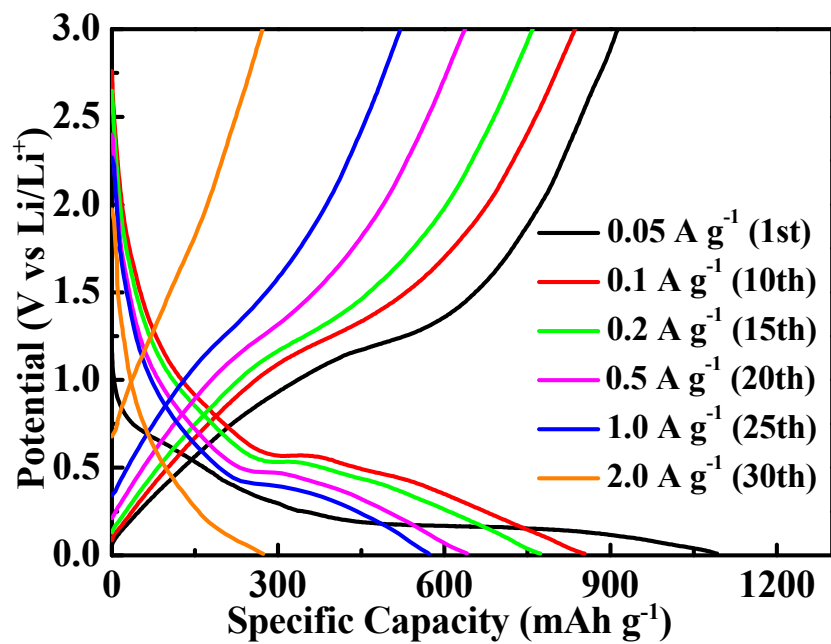


Figure S5. Charge-discharge profiles of MnO-Ni10@C electrodes at different current densities.

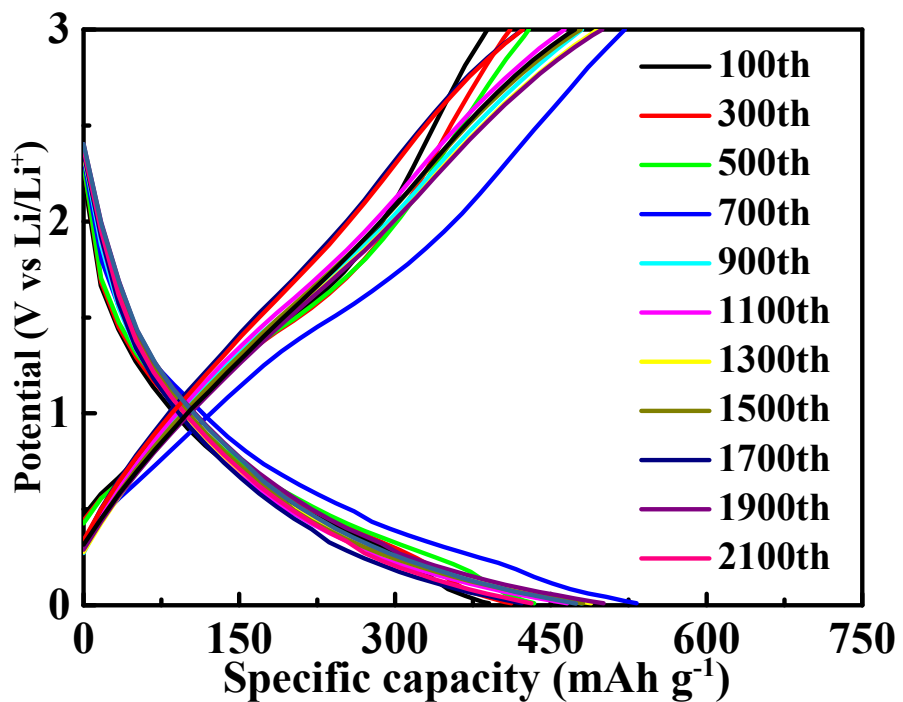


Figure S6. The corresponding selected charge-discharge profiles of MnO-Ni10@C at 1.0 A g⁻¹ for a ultralong cycle life of 2100 cycles.

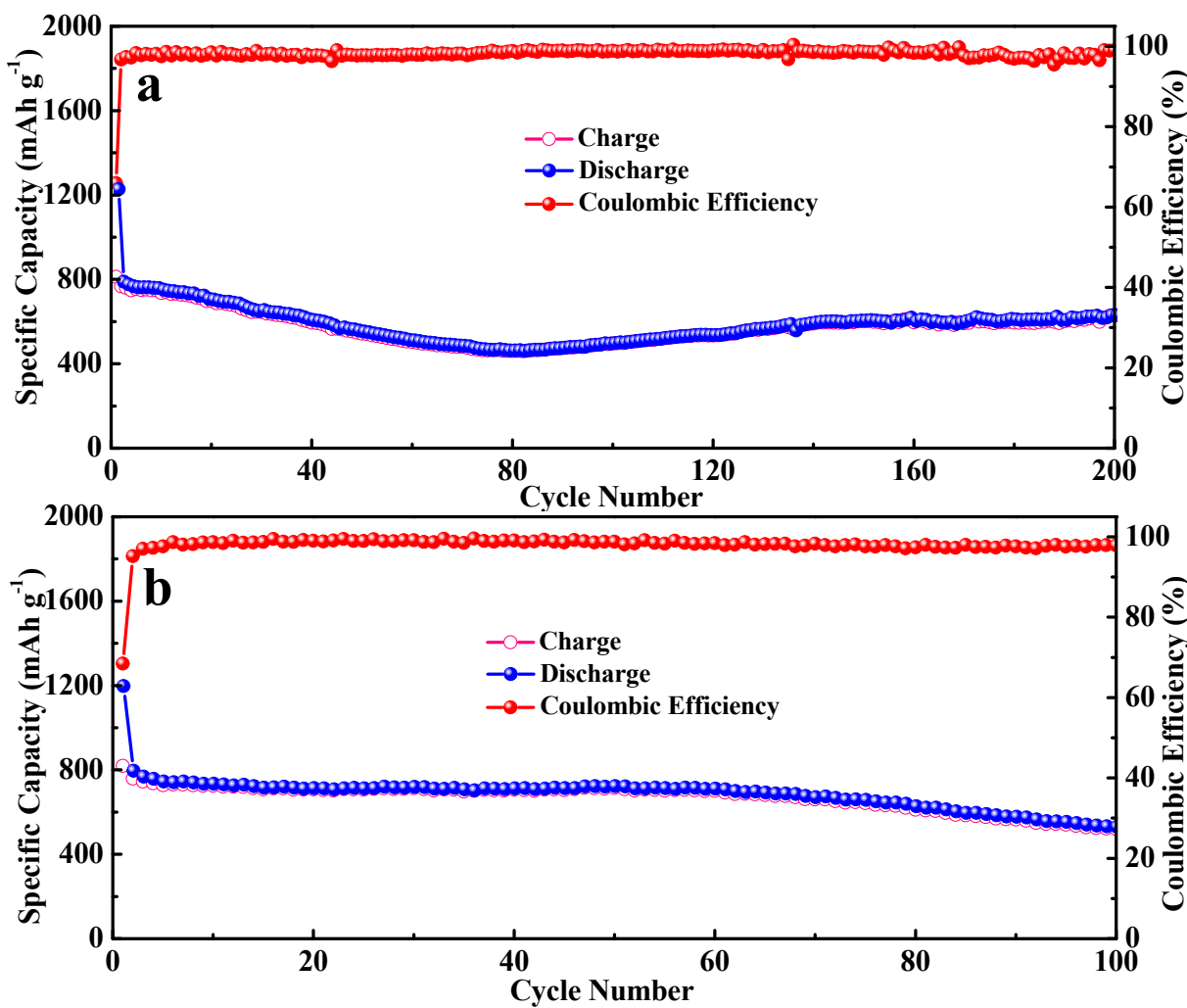


Figure S7. Cycling performance and coulombic efficiency of MnO-Ni5@C (a) and MnO-Ni15@C (b) electrodes at current density of 0.1 A g^{-1} .

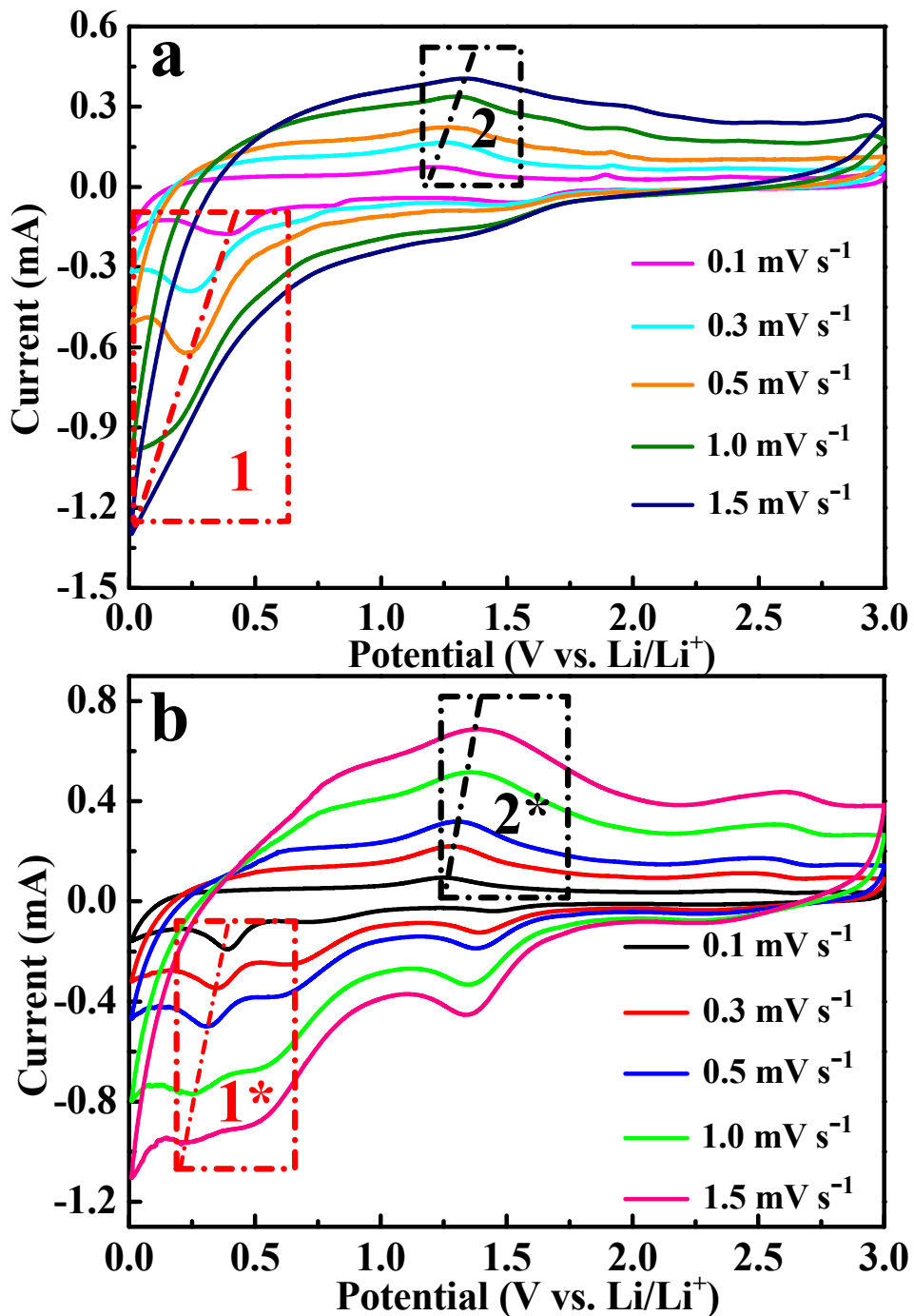


Figure S8. CV curves at different scan rates from 0.1-1.5 mV s⁻¹ of MnO-Ni0@C (a) and MnO-Ni10@C (b) electrodes.

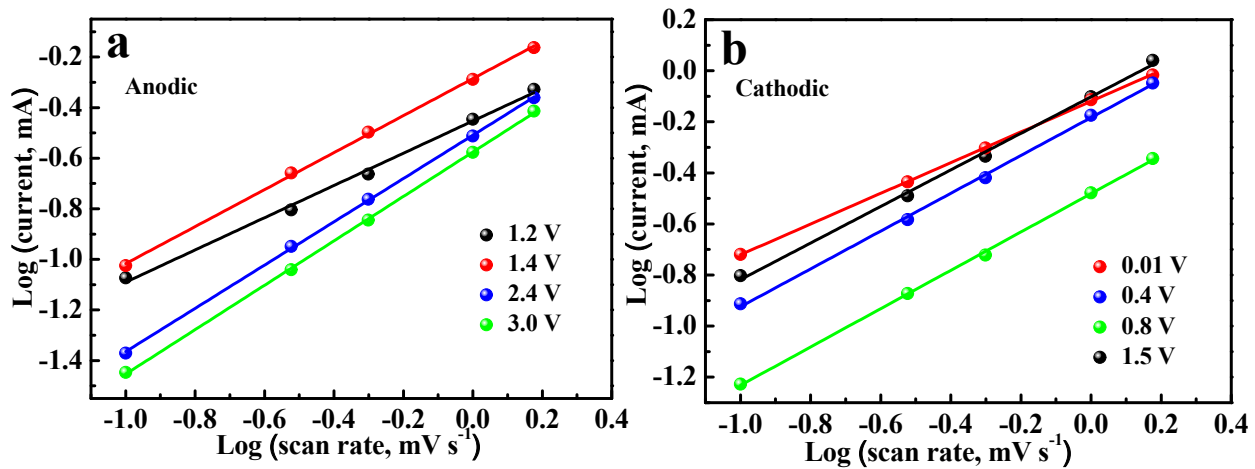


Figure S9. Current responses plotted against different scan rates of MnO-Ni10@C electrodes at different potentials for anodic scans (a) and cathodic scans (b).

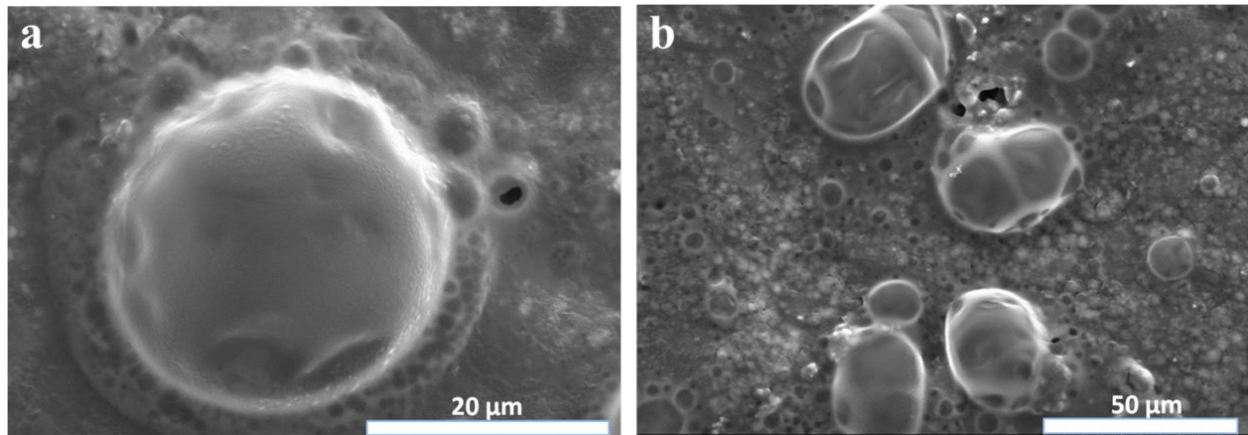
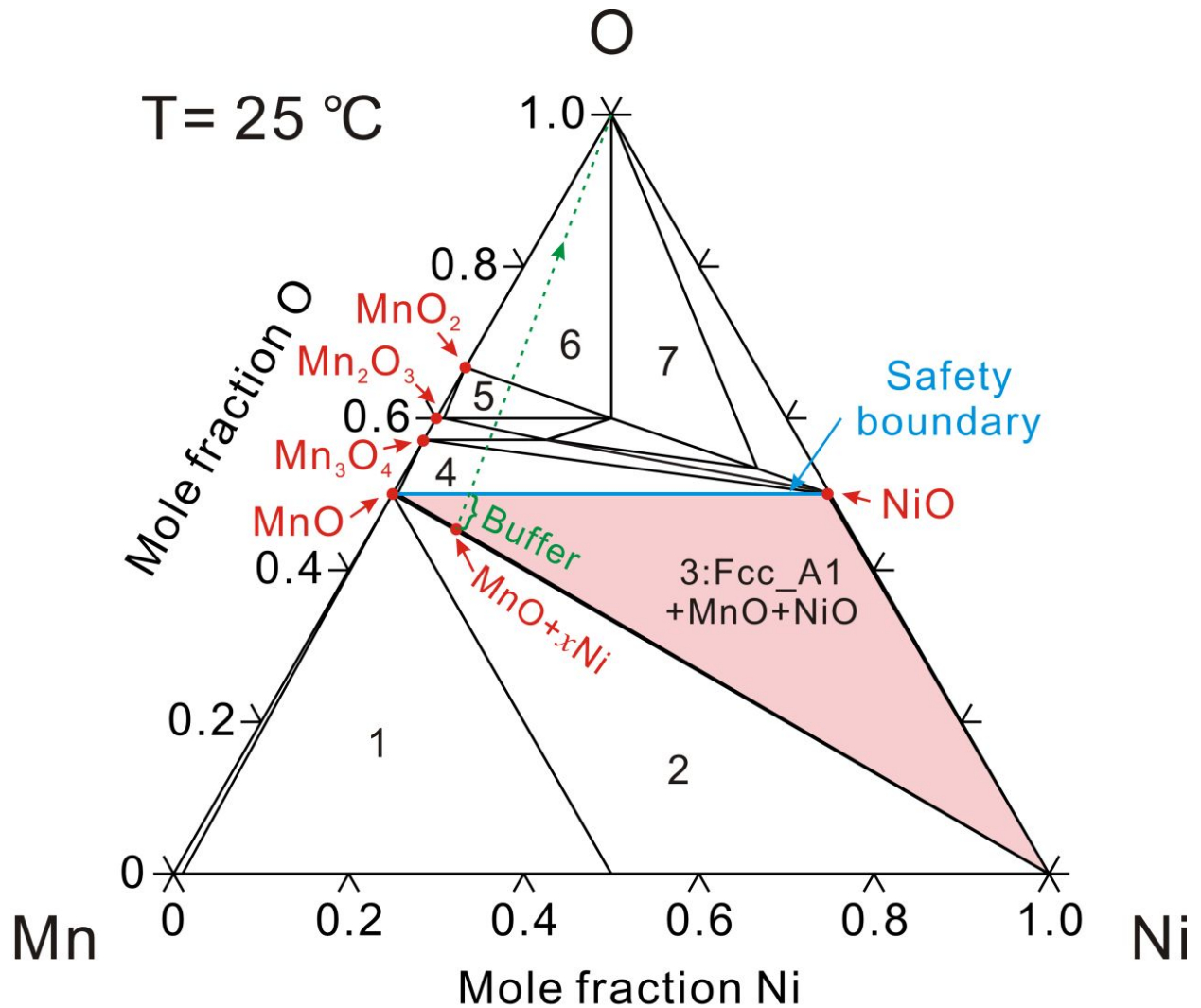


Figure S10. SEM images of MnO-Ni5@C (a) and MnO-Ni15@C (b) electrodes after 200 and 100 cycles, respectively.



- | | |
|--|--|
| 1: $\alpha\text{Mn} + \alpha\text{MnNi} + \text{Halite}$ | 5: $\text{Mn}_2\text{O}_3 + \text{MnO}_2 + \text{NiMnO}_3$ |
| 2: $\text{Fcc_A1} + \alpha\text{MnNi} + \text{MnO}$ | 6: $\text{MnO}_2 + \text{Gas} + \text{NiMnO}_3$ |
| 4: $\text{Mn}_3\text{O}_4 + \text{MnO} + \text{NiO}$ | 7: $\text{Ni}_6\text{MnO}_8 + \text{Gas} + \text{NiMnO}_3$ |

Figure S11. The calculated room temperature phase diagram of Ni-Mn-O system. The dashed line is the oxidation direction of the $\text{MnO}+\text{xNi}$ alloys.

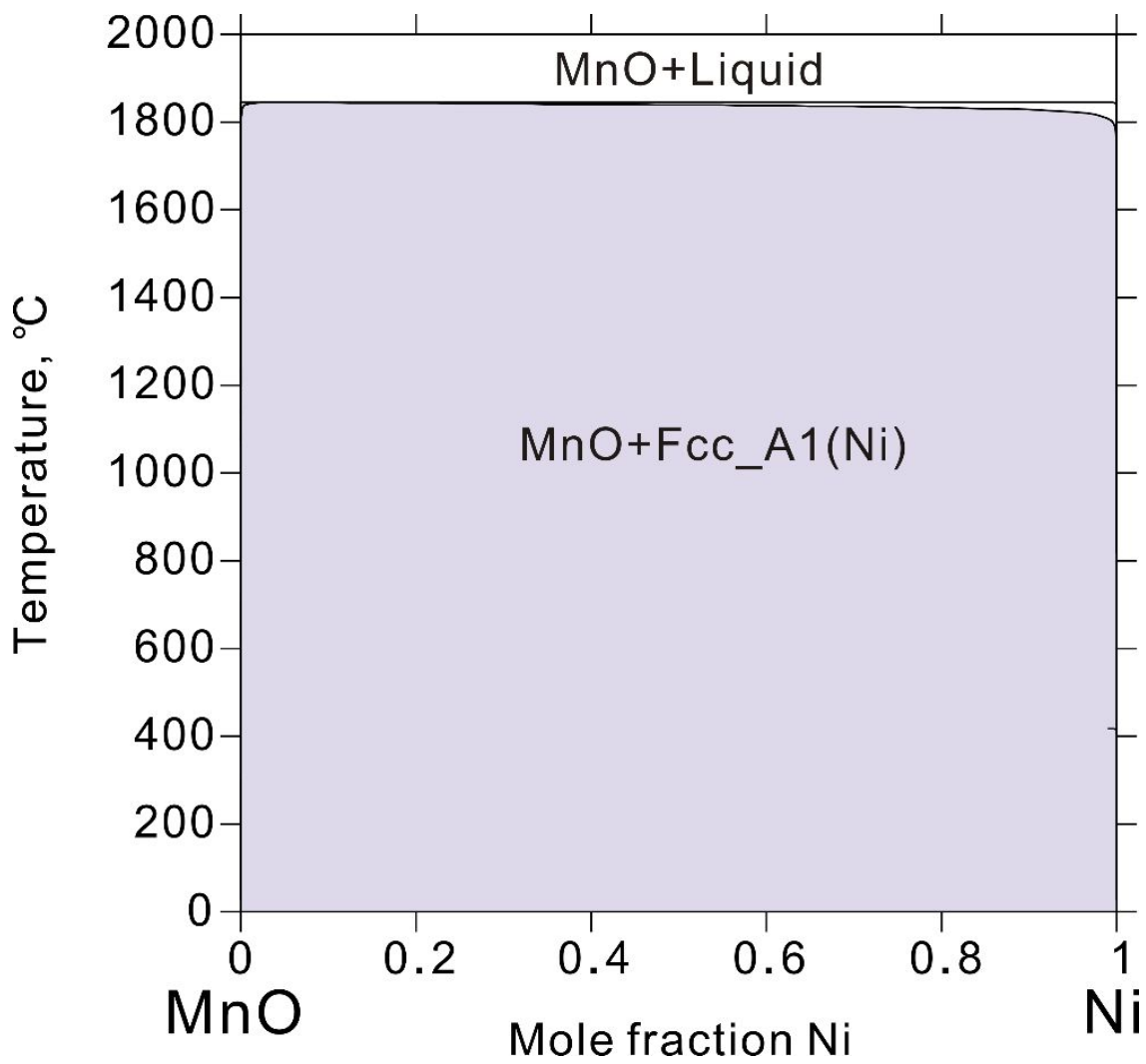


Figure S12. Calculated MnO-Ni vertical section of the Ni-Mn-O system.

Table S1. Comparisons of the electrochemical performance of the transition metal oxides electrodes.

MnO-based Materials	Current Density [A g ⁻¹]	Cycle Number	Initial Value (the 2 th cycle)	Crest Value [mAh g ⁻¹]	Retention of Discharge Capacity	References
[mAh g ⁻¹]						
MnO@Mn ₃ O ₄	0.2	300	748	1300	173.79%	1
MnO/C-N	0.5	500	582	783	134.53%	2
CNT/Co ₃ O ₄	0.1	100	900	1200	133.33%	3
Co ₃ O ₄	1.0	1000	762	1910	250.65%	4
MnO@Graphene	0.2	100	805	1202	149.32%	5
RGO-MnO-RGO	2.0	500	600	1269.2	211.53%	6
MnO/carbon matrix	0.1	100	760	952	125.26%	7
MnO/C	1.0	1000	890	1212	136.18%	8
MnO/N-Doped C	0.1	200	1231.1	1699	138%	9
MnO /Carbon	0.5	170	420	1467.	349.29%	10
MnO Nanoparticles	5.0	5000	825	939	113.82%	11
MnO/C nanowires	0.1	100	635	832	131.02%	12
MnO on Graphene	0.2	150	890.7	2014.1	226.13%	13
Nano-MnO/C	0.1	200	895	1082	120.89%	14
MnO@C Nanowires	0.5	200	650	801	123.23%	15
MnO/Carbon	0.5	300	735	1453	197.69%	16
MnO@C	0.1	270	673	1450.5	215.53%	17
MnO/N-doped C	0.5	100	795	982	123.52%	18
This work	0.1	200	820	832	101.46%	

Notes and references

- (1) Chu, Y. T.; Guo, L. Y.; Xi, B. J.; Feng, Z. Y.; Wu, F. F.; Lin, Y.; Liu, J. C.; Sun, D.; Feng, J. K.; Qian, Y. T.; Xiong, S. L. Embedding MnO@Mn₃O₄ Nanoparticles in an N-Doped-Carbon Framework Derived from Mn-Organic Clusters for Efficient Lithium Storage. *Adv. Mater.* **2018**, *30*, 1704244.
- (2) Zhu, G. Y.; Wang, L.; Lin, H. N.; Ma, L. B.; Zhao, P. Y.; Hu, Y.; Chen, T.; Chen, R. P.; Wang, Y. R.; Tie, Z. X.; Liu, J.; Jin, Z. Walnut-Like Multicore-Shell MnO Encapsulated Nitrogen-Rich Carbon Nanocapsules as Anode Material for Long-Cycling and Soft-Packed Lithium-ion Batteries. *Adv. Funct. Mater.* **2018**, *28*, 1800003.
- (3) Chen, Y. J.; Wang, Y. S.; Wang, Z. P.; Zou, M. C.; Zhang, H.; Zhao, W. Q.; Yousaf, M.; Yang, L.; Cao, A.; Han, R. P. S. Densification by Compaction as an Effective Low-Cost Method to Attain a High Areal Lithium Storage Capacity in a CNT@Co₃O₄ Sponge. *Adv. Energy Mater.* **2018**, *8*, 1702981.
- (4) Hou, C. X.; Hou, Y.; Fan, Y. Q.; Zhai, Y. J.; Wang, Y.; Sun, Z. Y.; Fan, R. H.; Dang, F.; Wang, J. Oxygen Vacancy Derived Local Build-in Electric Field in Mesoporous Hollow Co₃O₄ Microspheres Promotes High-Performance Li-ion Batteries. *J. Mater. Chem. A* **2018**, *6*, 6967-6976.
- (5) Zhang, Y.; Chen, P. H.; Gao, X.; Wang, B.; Liu, H.; Wu, H.; Liu, H. K.; Dou, S. X. Nitrogen-Doped Graphene Ribbon Assembled Core-Sheath MnO@Graphene Scrolls as Hierarchically Ordered 3D Porous Electrodes for Fast and Durable Lithium Storage. *Adv. Funct. Mater.* **2016**, *26*, 7754-7765.
- (6) Yuan, T. Z.; Jiang, Y. Z.; Sun, W. P.; Xiang, B.; Li, Y.; Yan, M.; Xu, B.; Dou, S. X. Ever-Increasing Pseudocapacitance in RGO-MnO-RGO Sandwich Nanostructures for Ultrahigh-

- Rate Lithium Storage. *Adv. Funct. Mater.* **2016**, *26*, 2198-2206.
- (7) Yang, C. X.; Gao, Q. M.; Tian, W. Q.; Tan, Y. L.; Zhang, T.; Yang, K.; Zhu, L. H. Superlow Load of Nanosized MnO on a Porous Carbon Matrix from Wood Fibre with Superior Lithium Ion Storage Performance. *J. Mater. Chem. A* **2014**, *2*, 19975-19982.
- (8) Xiao, Y. C.; Xu, C. Y.; Wang, P. P.; Fang, H. T.; Sun, X. Y.; Ma, F. X.; Pei, Y.; Zhen, L. Encapsulating MnO Nanoparticles within Foam-Like Carbon Nanosheet Matrix for Fast and Durable Lithium Storage. *Nano Energy* **2018**, *50*, 675-684.
- (9) Xiao, Y.; Wang, X.; Wang, W.; Zhao, D.; Cao, M. H. Engineering Hybrid Between MnO and N-Doped Carbon to Achieve Exceptionally High Capacity for Lithium-ion Battery Anode. *ACS Appl. Mater. Interfaces* **2014**, *6*, 2051-2058.
- (10) Xiao, Y.; Cao, M. H. Carbon-Anchored MnO Nanosheets as an Anode for High-Rate and Long-Life Lithium-ion Batteries. *ACS Appl. Mater. Interfaces* **2015**, *7*, 12840-12849.
- (11) Wang, S. B.; Xing, Y. L.; Xu, H. Z.; Zhang, S. C. MnO Nanoparticles Interdispersed in 3D Porous Carbon Framework for High Performance Lithium-ion Batteries. *ACS Appl. Mater. Interfaces* **2014**, *6*, 12713-12718.
- (12) Wang, J. G.; Zhang, C. B.; Jin, D. D.; Xie, K. Y.; Wei, B. Q. Synthesis of Ultralong MnO/C Coaxial Nanowires as Freestanding Anodes for High-Performance Lithium Ion Batteries. *J. Mater. Chem. A* **2015**, *3*, 13699-13705.
- (13) Sun, Y. M.; Hu, X. L.; Luo, W.; Xia, F. F.; Huang, Y. H. Reconstruction of Conformal Nanoscale MnO on Graphene as a High-Capacity and Long-Life Anode Material for Lithium Ion Batteries. *Adv. Funct. Mater.* **2013**, *23*, 2436-2444.
- (14) Liu, B.; Hu, X. L.; Xu, H. H.; Luo, W.; Sun, Y. M.; Huang, Y. H. Encapsulation of MnO Nanocrystals in Electrospun Carbon Nanofibers as High-Performance Anode Materials for

- Lithium-ion Batteries. *Sci. Rep.* **2014**, *4*, 4229.
- (15) Li, X. W.; Xiong, S. L.; Li, J. F.; Liang, X.; Wang, J. Z.; Bai, J.; Qian, Y. T. MnO@ Carbon Core-Shell Nanowires as Stable High-Performance Anodes for Lithium-ion Batteries. *Chem, -Eur. J.* **2013**, *19*, 11310-11319.
- (16) Jiang, X. J.; Yu, W.; Wang, H.; Xu, H. Y.; Liu, X. Z.; Ding, Y. Enhancing the Performance of MnO by Double Carbon Modification for Advanced Lithium-ion Battery Anodes. *J. Mater. Chem. A* **2016**, *4*, 920-925.
- (17) Hou, C. X.; Tai, Z. X.; Zhao, L. L.; Zhai, Y. J.; Hou, Y.; Fan, Y. Q.; Dang, F.; Wang, J.; Liu, H. K. High Performance MnO@ C Microcages with a Hierarchical Structure and Tunable Carbon Shell for Efficient and Durable Lithium Storage. *J. Mater. Chem. A* **2018**, *6*, 9723-9736.
- (18) Gu, X.; Yue, J.; Chen, L.; Liu, S.; Xu, H. Y.; Yang, J.; Qian, Y. T.; Zhao, X. B. Coaxial MnO/N-Doped Carbon Nanorods for Advanced Lithium-ion Battery Anodes. *J. Mater. Chem. A* **2015**, *3*, 1037-1041.